UDK 669.721.5:66.065.53
Original scientific article/Izvirni znanstveni članek

ISSN 1580-2949
MTAEC9, 56(4)351(2022)

EFFECT OF UPSETTING-EXTRUSION-UPSETTING ON THE RECRYSTALLIZATION OF AN Mg-9Gd-4Y-2Zn-0.5Zr ALLOY

VPLIV POSEBNEGA POSTOPKA IZTISKOVANJA NA REKRISTALIZACIJO MAGNEZIJEVE ZLITINE VRSTE Mg-9Gd-4Y-2Zn-0.5Zr

Zhikang Peng, Leichen Jia, Guanshi Zhang, Zhimin Zhang, Qiang Wang, Jianmin Yu, Jian Xu, Yong Xue*

School of Materials Science and Engineering, North University of China, Taiyuan 030051, China

Prejem rokopisa – received: 2022-01-17; sprejem za objavo – accepted for publication: 2022-05-09

doi:10.17222/mit.2022.372

In this study, the effect of upsetting-extrusion-upsetting (UEU) on the microstructure of an Mg-9Gd-4Y-2Zn-0.5Zr alloy and on dynamic recrystallization (DRX) was investigated. The results showed that after UEU, DRX occurred in the Mg-9Gd-4Y-2Zn-0.5Zr alloy. Namely, the grain refinement at the cross-sectional edges of UEU specimens was significant, with the grain size being refined from 8.27 μm in the necking region to 6.57 μm. Grain refinement is mainly caused by DRX where the long-period stacking order (LPSO) phase stimulates DRX around the grain boundaries through a particle-stimulated nucleation mechanism. DRX grains play an important role in weakening the texture by offsetting the severely deformed structure of deformed grains.

Keywords: magnesium alloy, upsetting-extrusion-upsetting, microstructure, texture

V članku avtorji opisujejo vpliv rekristalizacije na mikrostrukturo zlitine Mg-9Gd-4Y-2Zn-0,5Zr, ki je nastala med procesom dinamične rekristalizacije (DRX) pri izvajanju posebnega postopka njenega iztiskovanja (UEU; angl.: upsetting-extrusion-upsetting). Rezultati raziskave so pokazali, da je med postopkom iztiskovanja v magnezijevi zlitini Mg-9Gd-4Y-2Zn-0,5Zr potekal proces dinamične rekristalizacije. Pri tem je prišlo do znatnega zmanjšanja velikosti kristalnih zrn na robovih UEU preizkušancev in sicer na 8,27 μm in v področju zoženja na 6,57 μm. Zmanjšanje kristalnih zrn je predvsem posledica dinamične rekristalizacije med katero je faza z urejenostjo zloga dolgega dosega (LPSO; angl.: long-period stacking order) stimulirala dinamično rekristalizacijo okoli kristalnih mej z mehanizmom nukleacije delcev druge faze. Kristalna zrna nastala zaradi dinamične rekristalizacije igrajo pomembno vlogo pri slabšanju teksture preizkušancev z močno deformirano strukturo kristalnih zrn.

Ključne besede: zlitina na osnovi magnezija, postopek iztiskovanja, mikrostruktura, tekstura

1 INTRODUCTION

Magnesium alloys are currently the lightest metal-based structural materials available and they have great potential for use in the automotive and aerospace industries due to their low density, high specific strength, high specific stiffness, good machinability and ease of recycling.[1–3] However, most of the magnesium structural parts are produced by die-casting,[4] but a cast magnesium alloy is coarse, having low strength and poor plasticity so that the product shape, size and application range are greatly restricted. Compared with cast magnesium alloys, the plastic processing of deformed magnesium alloys including grain refinement, thus allowing excellent mechanical properties, is more suitable for the production of large structural parts, and meets the requirements of structural diversification, showing massive potential for development.[5] Severe plastic deformation (SPD) can effectively refine the grain size and allow us to obtain a complete large-size block specimen; by controlling the microstructure during the deformation process, a block material with high strength and high plasticity can be obtained at the same time. Severe plastic deformation (SPD) is suitable for the preparation of large homogeneous fine-grained alloys.[6]

SPD has long been considered as one of the best processes for refining the grain structure and alloys have been significantly refined with repetitive SPD,[7] but this requires multiple heating, which consumes a lot of valuable energy. With the worldwide energy shortage, energy conservation and utilization efficiency have become imminent. According to some previous studies on the multi-pass SPD of magnesium alloys, i.e., the ones by Meng, Zhang et al.,[7,8] the cumulative deformation of three passes was only 4.11 and 4.04, respectively. On the contrary, the authors of this article use a new process, UEU, which combines two passes of conventional upsetting and one pass of conventional extrusion allowing intense deformation. A single strain can reach 4.00 and only one heating is required, which can save energy significantly. At the same time, it can effectively avoid the grain growth caused by a long multiple-strain heat treatment. Taking the high-strength Mg-9Gd-4Y-2Zn-0.5Zr

*Corresponding author's e-mail:
yongxue395@163.com

alloy[9] as the object examined from different perspectives, we observed the microstructural characteristics of different parts of the alloy after UEU, and analysed the microstructure evolution law and deformation mechanism during the extrusion process. The effect of UEU on the recrystallization of different regions of the alloy microstructure was studied to provide a reference for optimizing the UEU process and preparing fine-grained magnesium alloys.

2 EXPERIMENTAL PART

In this experiment, the Mg-9Gd-4Y-2Zn-0.5Zr alloy, supplied by Silverlight Magnesium Co. Ltd., was used as a cast billet with a diameter of 32 mm and a length of 150 mm. It was homogenised at 520 °C for 24 h, then quenched in hot water (70 °C) to obtain a homogeneous initial ingot.

The UEU process is shown in **Figure 1** where the upsetting cavity has a diameter of 103 mm, the extrusion split-flap cavity has a diameter of 38 mm, and the extrusion/upsetting split-flap cavity has a diameter of 53 mm. From Equation (1), the cumulative strain for upsetting and extrusion can be calculated as 1.33, 3.33 and 4.00, respectively.[10]

$$\varepsilon = 4n \ln\left(\frac{2R}{d}\right) \tag{1}$$

Here, n is the number of process orifices; $2R$ is the diameter of the upsetting cavity; d is the diameter of the extrusion cavity.

Before UEU, the blanks and dies were preheated to a uniform temperature and heated for an isothermal time of 1 h. The samples were lubricated with an oil-based graphite lubricant. The UEU process was carried out in a 630 kN hydraulic press at a speed of 5 mm/s; the temperature was reduced from 450 °C to 430 °C after one-pass UEU. Different regions of a one-pass UEU specimen were selected for a microstructure analysis and cut from the UEU specimen. These samples were sandpapered and polished on a stepless speed polisher, then etched for 5 s in an etching solution consisting of 2 mL of distilled water, 2 mL of glacial acetic acid, 1 g of picric acid and 14 mL of alcohol. The microstructure was examined in the ED direction using an optical microscope (OM, Zeiss Axio lmager A1m) and a scanning electron microscope (SEM, Hitachi SU5000) equipped with an energy spectrometer (EDX). An X-ray diffraction (XRD, Smart Lab SE) analysis was performed on the samples using the 2θ diffraction angle.

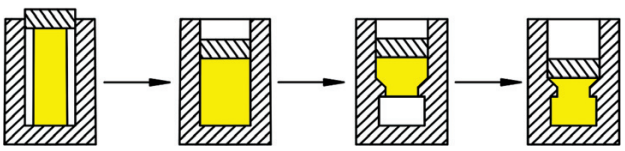

Figure 1: Principle of the UEU processing

An electron backscatter diffraction analysis (EBSD) was performed using a scanning electron microscope (SEM, Hitachi SU5000) equipped with an EDAX-TSL EBSD system with 20 kV, a 70° tilt angle and a working distance of 15 mm. Prior to the EBSD observation, the sample quality was improved by removing the residual stress layer by running the Leica EM Res 102 ion thinning instrument at 6.5 kV for 35 min, which further eliminated experimental errors and thus guaranteed the accuracy of the EBSD measurements. Data processing was carried out using orientation imaging microscopy (OIM) software 7.3 to analyse the grain size, grain boundary angles, polar diagrams, etc.

3 RESULTS AND DISCUSSION

3.1 Evolution of the microstructure

In order to study the evolution of the structure during the repetitive pier extrusion process, the Mg-9Gd-4Y-2Zn-0.5Zr alloy was pier extruded in one pass at 450 °C. The specific sampling areas for metallographic samples are shown in **Figure 2** where region A is the necking region, region B is the core region, region C is the $R/2$ region, region D is the bend region, region E is the upper-edge region and region F is the lower-edge region.

Figure 3 shows the microstructure of the longitudinal section of the concave die area. It is evident that the alloy deformation in the extrusion area is similar to that of the positive extrusion after the upsetting of the necking region, and the arrow in **Figure 3** shows the distribution of the extrusion flow line.

Figure 4 shows OM micrographs of different parts of the alloy after UEU and their corresponding backscattered electron (BSE) images. It can be found that the LPSO phase tends to be distributed in a streamline pattern along the extrusion direction, and some of the bulk LPSO phase breaks and bends at a certain angle. **Figure 5** shows XRD patterns of the organization of different parts of the alloy after the UEU deformation. **Figure 4a** shows the longitudinal cross-sectional microstructure of

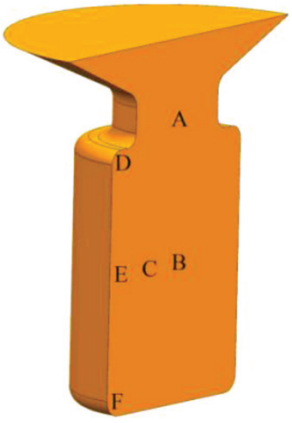

Figure 2: Diagram of the specific sampling regions for metallographic samples

the region A specimen. **Figure 4c** shows the microstructure of the longitudinal section of the specimen from region B. As can be seen in **Figure 4d**, the LPSO phase is elongated along the extrusion direction having a jagged boundary. The microstructure of the longitudinal section of the specimen from region D shown in **Figure 4g** is dominated by grains with large deformations. **Figure 4i** shows the microstructure of the longitudinal section at the edge of the E region where complete DRX occurred, and the organization is more homogeneous and mainly composed of fine equiaxed crystals. This is mainly due to the fact that the bulk LPSO phase with high Young's modulus provides ideal sites for the nucleation of DRX grains during the deformation process through particle-stimulated nucleation (PSN) mechanism, which promotes dynamic recrystallization (DRX). On the other hand, in addition to the grain refinement, there are many dynamic precipitations, namely the β-phases (Mg 5(Gd, Y, Zn)) around the DRX grains. These β-phases can inhibit the grain boundary migration and retard the grain growth. **Figure 4k** shows the microstructure of the longitudinal section at the bottom edge of the specimen. As shown in **Figure 4k**, most grains are coarse, with many tiny equiaxed crystals interspersed between the coarse and large grains.

During the alloy deformation after one-pass UEU, no new phases were formed in different regions of the microstructure, but the content changed (**Figure 5**). After the one-pass process, the grains of the alloy were refined, and the organization of the E region was the most obvious **(Figure 6f**). The typical bimodal microstructure was not difficult to find at the original coarse grain boundaries. Here, it can be observed that the large coarse grains are elongated along the ED direction, and chain-like DRX grains appear at the trigonal grain boundaries (GBs) of the coarse grains. This indicates that discontinuous dynamic recrystallization[11] occurred after one-pass UEU. GBs have a significant hindering effect on the movement of dislocations.[12,13] The movement of dislocations therefore quickly causes stress concentration and large deformation of GBs.

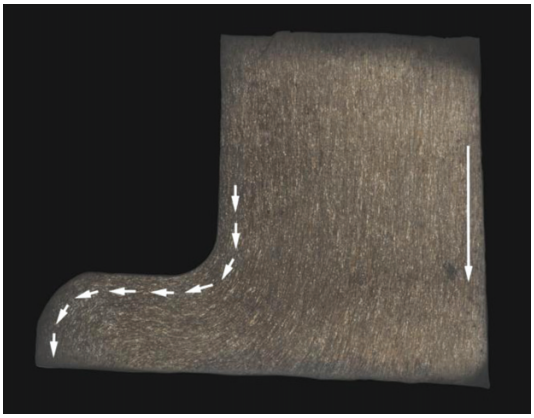

Figure 3: Longitudinal-section microstructure of the die area of an UEU sample

As the pegging effect of these particles on the sliding of GBs inhibits the growth of DRX grains during UEU, the proportion of DRX grains continues to increase as UEU proceeds, while the coarse grains are consumed more efficiently and their size is refined from 13.21 μm in the A region to 6.64 μm in the B region. The microstructure becomes more homogeneous. Although some of the original coarse grains remain intact after UEU, more grains are refined into equiaxed grains, contrasting the ones in the A region, and significant changes in the microstructure can be observed.

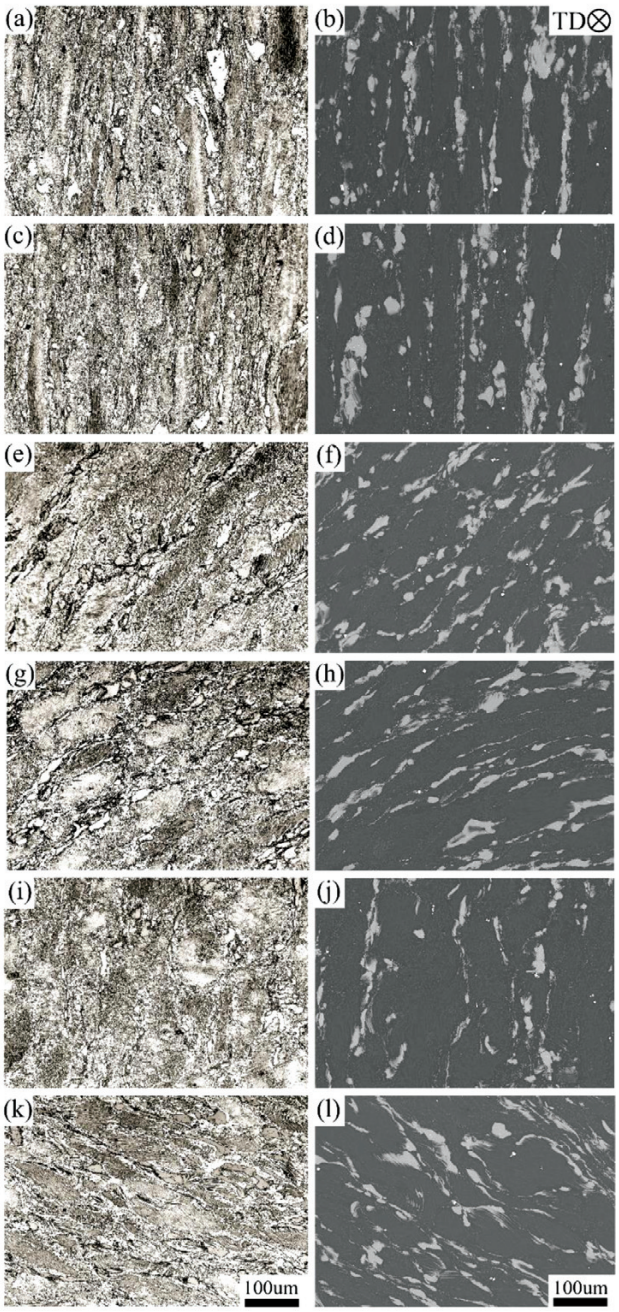

Figure 4: Microstructure images of regions after UEU at 450 °C: a) A-OM, b) A-BSE, c) B-OM, d) B-BSE, e) C-OM, f) C-BSE g) D-OM, h) D-BSE i) E-OM, j) E-BSE, k) F-OM, l) F-BSE

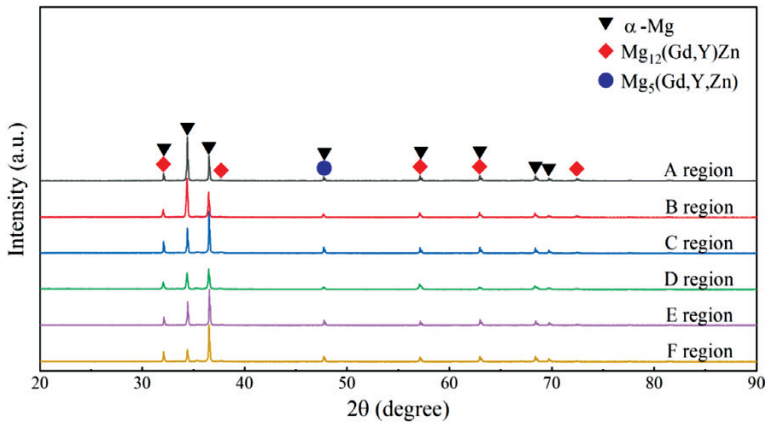

Figure 5: XRD analysis of different sampling regions

Table 1: Grain-size distribution for different regions of the alloy after one-pass UEU processing

Region	A	B	C	D	E	F
Average grain size (μm)	8	7	8	9	7	30
Standard deviation	13.21	6.64	9.44	11.83	5.27	31.23

Figure 6 shows the microstructure evolution in the region of the specimen cross-section from the centre to the edge. The same or similar colour indicates the same or similar grain orientation, and the black part indicates the LPSO phase. As shown on **Figure 6** and **Table 1**, there is a layer of fine equiaxed grains close to the edge, adjacent to the extrusion cylinder wall. In the same cross-section (where regions B, C and E constitute the same cross-sectional area), the grains coarsen as the distance from the edge increases. At the same time, the volume fraction of refined grains in the microstructure gradually decreases, and the volume fraction of coarse grains gradually increases. However, after a specific limit is reached, the coarse grains gradually change into uniform fine equiaxed crystals as the distance from the edge increases, and the volume fraction of refined grains in the microstructure gradually increases. The volume fraction of coarse grains gradually decreases.

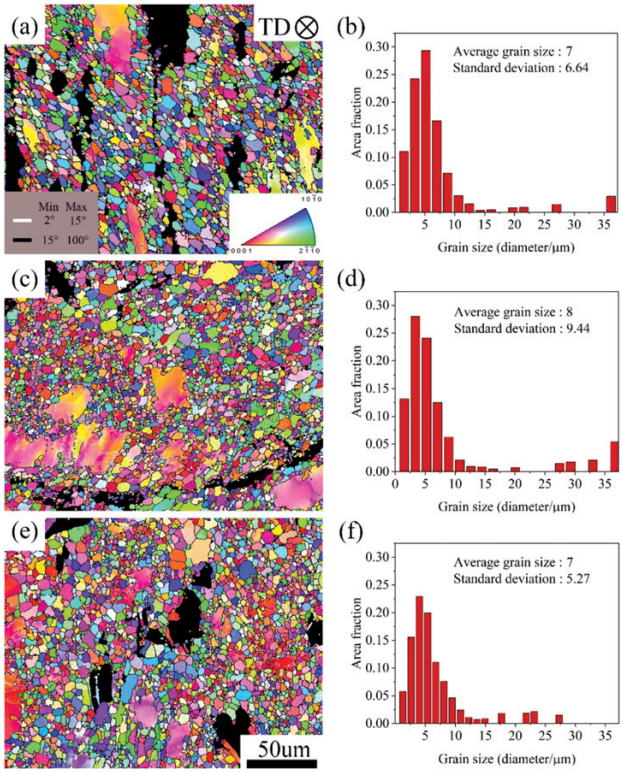

Figure 6: EBSD orientation maps of the alloy after UEU at 450 °C: a) B region, b) C region, e) E region and their corresponding grain sizes (b, d, f)

3.2 Grain boundary characteristics

Table 2: Dislocation-angle distribution for different regions of the alloy after one-pass UEU

	Angle deformation		
	2°–5°	5°–15°	15°–180°
A region (%)	13	3	83
B region (%)	10	3	88
C region (%)	19	4	77
D region (%)	13	2	85
E region (%)	15	4	81
F region (%)	21	4	75

Figure 7 shows the grain-orientation distribution and the variation in the dislocation angle of the alloy. The EBSD method was used to statistically investigate the grain-boundary angles of different regions of the prepared alloy. EBSD plots of the alloy after the UEU treatment at 450 °C are shown in **Figure 7**. In this case, grain boundaries with a dislocation angle of 0–15° are called low-angle grain boundaries (LAGB), while grain boundaries with a dislocation angle greater than 15° are called high-angle grain boundaries (HAGB). The number fractions (NFs) of LAGBs and HAGBs obtained by processing the dislocation angles in different regions of the alloy are shown in **Table 2** where the experimental error is ± 0.5 %.

Computer simulations of the repetitive extrusion process show that the material flows fastest in the central region, while on the thick side of the pier, near the inner

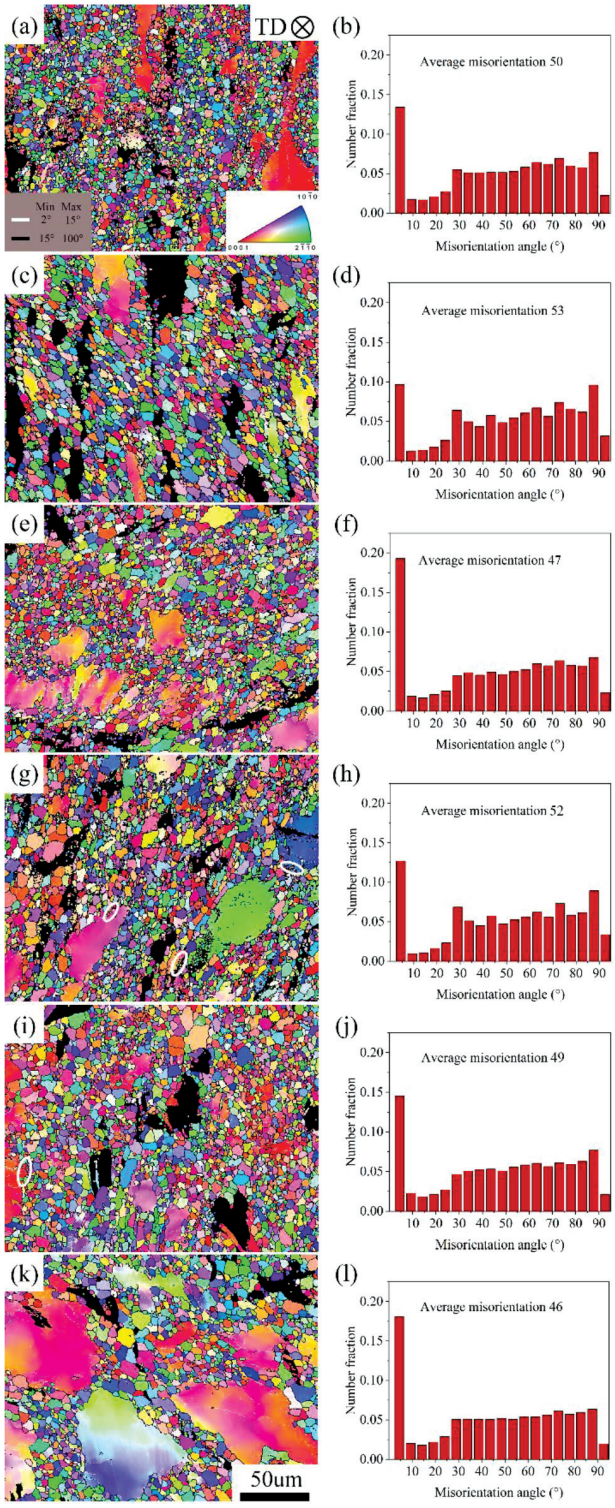

Figure 7: EBSD maps of the alloy after UEU at 450 °C: a) A region, c) B region, e) C region, g) D region, i) E region, k) F region and their corresponding dislocation angles (b, d, f, h, j, l)

wall of the extrusion barrel, the material moves the slowest. Although the material rheology is fastest in the central region on the rough pier side, it is limited by the amount of deformation, and the local area does not flow perpendicularly to the extrusion direction. In contrast, near the inner side of the extrusion barrel, although the material flows at a slower rate, the amount of deformation is more significant and can be observed to be significantly elongated along the extrusion direction. **Figure 8** shows the kernel average misorientation (KAM) map of a sample. When the material acquires a higher amount of deformation, dense dislocations in the as-extruded sample are mainly concentrated inside the deformed grains, especially at the grain boundaries adjacent to the recrystallized grains (**Figure 8d**). **Figures 8e** and **8f** show uniform low-density dislocations, attributed to the formation of DRXed grains that consumed numerous dislocations. On the other hand, when the amount of deformation obtained by the material is small, the dislocation density is lower during plastic deformation (**Figure 8b**), so recrystallization is less likely to occur in the central region.

Also, the atomic free energy is more considerable for magnesium alloys with small grain sizes when the deformation temperature is higher.[14] When the slip diffusion energy of grain boundaries is higher than the grain-boundary diffusion energy and the lattice diffusion energy, grain boundaries undergo a relative slip.[15] As can be seen in **Table 2**, with the UEU at 450 °C, due to the friction between the extrusion cylinder wall and the metal material, under the action of shear, certain dislocation networks at adjacent subgrain boundaries (white circles in **Figures 7g** and **7i**) with small orientation differences are formed by dissociating, disassembling and transferring to the other subgrain boundaries, resulting in the disappearance of subgrain boundaries and the merging of subgrain boundaries.[16] The gradual transformation to HAGBs occurs due to the continuous movement of dislocations to the new grain boundaries.[17] These grain boundaries absorb dislocations through migration, resulting in further consumption of subcrystals and the formation of refined, dynamically recrystallized grains.[18] Therefore, the grain size is smaller in the area immediately inside the extrusion barrel.

After the one-pass UEU at 450 °C, observing the change in the grain-colour distribution from the boundaries to the centre in **Figure 7**, it can be seen that the deformed grains are strongly deformed internally. It is not difficult to find that the HAGBs in **Figure 7** are mainly composed of part of the newly formed recrystallization and the original coarse grains, while the LAGBs are mainly found inside the original coarse grains[19] near the DRX grain boundaries where the grains are uniform and fine. The LAGBs form kink bands as a result of interfacial dislocations arising from the lattice distortion. During the deformation caused by UEU, the LAGB kink bands reduce the local stress concentration by absorbing the surrounding dislocations, which eventually transform into HAGBs.[20]

On the other hand, these LAGBs help refine and separate the original coarse grains in the blanks.[21] The distribution of dislocation angles is mainly represented by

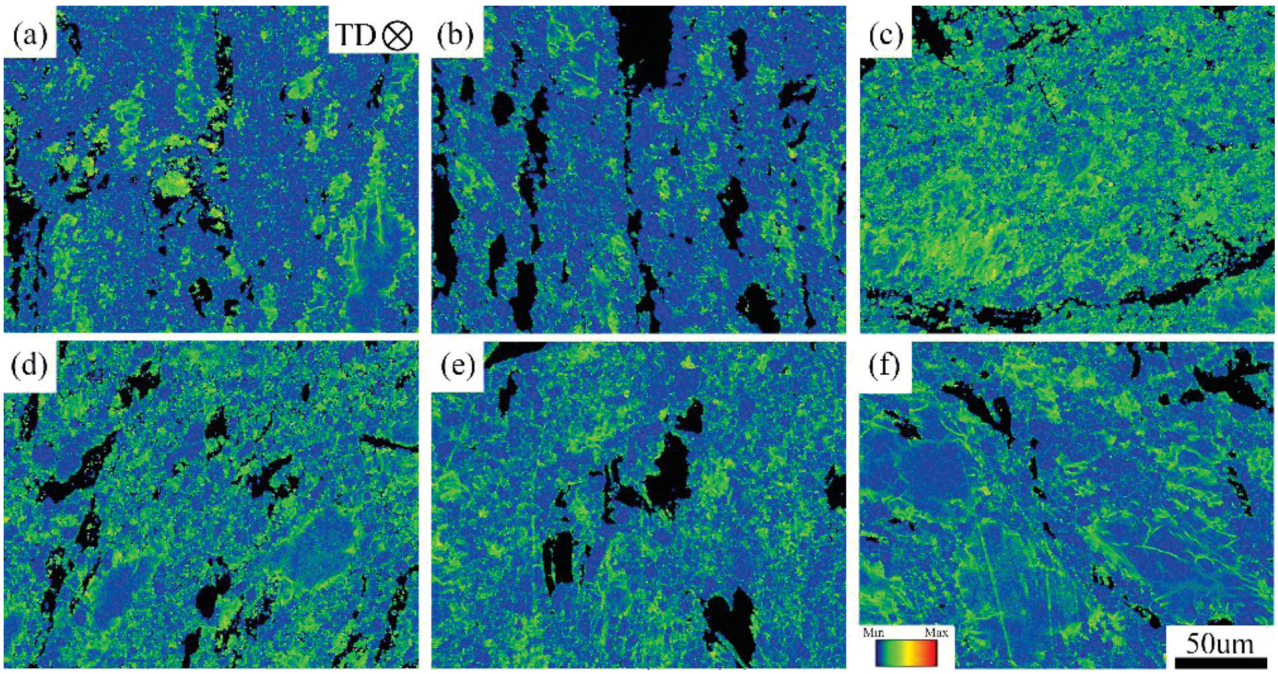

Figure 8: KAM maps of the alloy after UEU at 450 °C: a) A region, b) B region, c) C region, d) D region, e) E region, f) F region

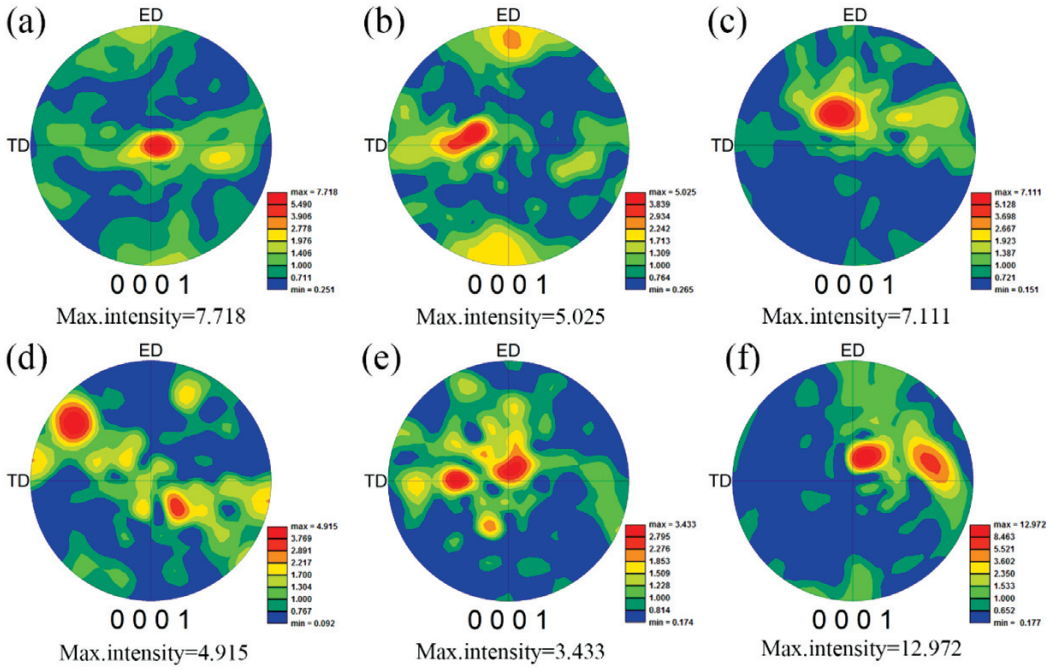

Figure 9: (0001) polar plot of different sampling regions on the ED-TD plane of the alloy after UEU: a) A region, b) B region, c) C region, d) D region, e) E region, f) F region

spikes with angles of less than 5° and many HAGBs (**Figure 7**). The values of NF of LAGBs gradually decrease with the increasing distance from the coarse grain ring, whereas the values of HAGBs gradually increase, and new grains containing HAGBs are formed due to the grain nucleation and growth at the original coarse-grain boundaries. Moreover, in the region of contact with the extruded cylinder wall, the outer metal is subjected to higher shear forces and acquires higher strains due to friction, which is most evident in the D region where secondary recrystallization is also more adequate. As the UEU process proceeds, the formation of new grains is accompanied by the formation of new LAGBs within them and the splitting of the original, coarser grains into several parts (**Figures 7c** and **7e**). It is noted that the NF values of LAGBs always appear throughout the evolution of LAGB microstructures with high NFs. This is referred

to as the characteristic dynamic recrystallization of continuous dynamic recrystallization (CDRX).

At the beginning of UEU, many refined grains can be observed at the original coarse-grain boundaries (**Figure 7i**). As the extrusion process continues, the original coarse grains are gradually broken by external forces, and DRX appears at the newly formed grain boundaries. This is because dislocations generally accumulate at grain boundaries when the grains are broken.[16] Stress concentration then occurs, and DRX appears, whereas the coarsening of the grains in **Figure 7k** is due to the growth of the grains after recrystallization. In terms of thermodynamic conditions, the growth of grains is such that the coarser the grains in a given volume of metal, the smaller is the total grain-boundary surface area and the lower is the total surface energy. As the coarsening of grains can reduce the surface energy[22] so that the metal or alloy is in a more stable, lower free energy state, the high-energy state tends to shift to lower energy automatically and the recrystallization process is unstable at large-angle grain boundaries. Hence, the situation from **Figure 7k** relies on the energy stored in dislocations to make the grains grow. This is also corroborated in **Figure 8**.

At the same time, along with the release of energy, the large-angle grain boundaries transform into small-angle grain boundaries, so the NF of LAGBs increases and that of HAGBs decreases in the lower edge region compared to the upper edge region, as shown in **Table 2**.

Figure 9 depicts the (0001) pole maps on the ED-TD plane of the alloy after the one-pass UEU at 450 °C for different sampling regions. The (0001) base surface of the extruded alloy is generally parallel to the base surface weave in the extrusion direction. However, after one pass of UEU, the (0001) base plane exhibits an angle of approximately 45° to the ED due to die binding in the D region where the metal flow is at an approximate angle of 45° to the extrusion direction (**Figure 7d**). At the same time, the C and F regions are shifted in the weave due to the extrusion direction, showing an angle with the metal-flow direction (**Figures 9c** and **9f**). The (0001) maximum intensity of the pole figure that appeared in the samples from the lower part of the edge was 12.972. Combining this result with the comparison from **Table 2**, it can be seen that as the volume fraction of DRX increases, the texture intensity gradually weakens. As the UEU deformation process is accompanied by an increase in the amount of accumulated strain, a decrease in the original coarse grains and an increase in the DRX grains, the direction of the DRX grains is more random, resulting in a decrease in the overall texture strength. DRX grains play an unparalleled role in weakening the structure by counteracting the severely deformed structure of the deformed grains.

4 CONCLUSIONS

1) In the UEU deformation process, the upsetting process is realized through grain boundary slip. No new phases are formed between different regions of a sample, but their content is changed. The grain refinement near the barrel wall is evident, and the high-efficiency grain refinement is mainly due to DRX.

2) In the UEU deformation process, due to the enhancement of the dynamic recrystallization process, the NF of LAGBs gradually decreases and that of HAGBs gradually increases. The new grains containing HAGBs are formed by the grain nucleation and growth at the original coarse-grain boundaries.

3) In the UEU deformation process, the texture of the magnesium alloy shifts due to the influence of the mould structure. The texture intensity gradually decreases as the volume fraction of DRX in the UEU process increases.

Acknowledgements

The study was supported by the National Natural Science Foundation of China (Grant No. 52075501).

Conflict of interest

All authors were involved in the study. The authors declare that there is no competitive economic interest.

5 REFERENCES

[1] Y. Yang, X. M. Xiong, J. Chen, X. D. Peng, D. L. Chen, F. S. Pan, Research advances in magnesium and magnesium alloys in 2020, J. Magnes. Alloy, 9 (**2021**), 705–747, doi:10.1016/j.jma.2021.04.001

[2] V. Balaji, V. K. B. Raja, K. Palanikumar, Ponshanmugakumar, N. Aditya, V. Rohit, Effect of heat treatment on magnesium alloys used in automotive industry: A review, Mater. Today: Proceedings, 46 (**2021**), 3769–3771, doi:10.1016/j.matpr.2021.02.017

[3] J. Rong, J. N. Zhu, W. L. Xiao, X. Q. Zhao, C. L. Ma, A high pressure die cast magnesium alloy with superior thermal conductivity and high strength, Intermetallics, 139 (**2021**), 107350, doi:10.1016/j.intermet.2021.107350

[4] N. P. Papenberg, S. Gneiger, I. Weißensteiner, P. J. Uggowitzer, S. Pogatscher, Mg-Alloys for forging magnesium applications – A review, Materials, 13 (**2020**), 1–61, doi:10.3390/ma13040985

[5] G. Song, Z. Diao, X. Lv, L. M. Liu, TIG and laser–TIG hybrid filler wire welding of casting and wrought dissimilar alloy, J. Manuf. Process., 34 (**2018**), 204–214, doi:10.1016/j.jmapro.2018.06.005

[6] G. S. Zhang, Z. M. Zhang, X. B. Li, Z. M. Yan, X. Che, J. M. Yu, Y. Z. Meng, Effects of repetitive upsetting-extrusion parameters on microstructure and texture evolution of Mg–Gd–Y–Zn–Zr alloy, J. Alloys Compd., 790 (**2019**), 48–57, doi:10.1016/j.jallcom.2019.03.207

[7] Y. Z. Meng, J. M. Yu, K. Liu, H. S. Yu, F. Zhang, Y. J. Wu, Z. M. Zhang, N. L. Luo, H. H. Wang, The evolution of long-period stacking ordered phase and its effect on dynamic recrystallization in Mg-Gd-Y-Zn-Zr alloy processed by repetitive upsetting-extrusion, J. Alloys Compd., 828 (**2020**), 154454, doi:10.1016/j.jallcom.2020.154454

[8] G. S. Zhang, Y. Z. Meng, F. F. Yan, Z. Gao, Z. M. Yan, Z. M. Zhang, Microstructure and texture evolution of Mg-RE-Zn alloy prepared by repetitive upsetting-extrusion under different decreasing temperature

degrees, J. Alloys Compd., 815 (**2020**), 152452, doi:10.1016/j.jallcom.2019.152452

[9] K. Luo, L. Zhang, G. H. Wu, W. C. Liu, W. J. Ding, Effect of Y and Gd content on the microstructure and mechanical properties of Mg–Y–RE alloys, J. Magnes. Alloy, 7 (**2019**), 345–354, doi:10.1016/j.jma.2019.03.002

[10] Y. Wu, S. H. Huang, Q. Chen, B. Feng, D. Y. Shu, Z. W. Huang, Microstructure and mechanical properties of copper billets fabricated by the repetitive extrusion and free forging process, J. Mater. Eng. Perform., 28 (**2019**), 2063–2070, doi:10.1007/s11665-019-03898-3

[11] Q. D. Wang, Y. J. Chen, M. P. Liu, J. B. Lin, H. J. Roven, Microstructure evolution of AZ series magnesium alloys during cyclic extrusion compression, Mater. Sci. Eng. A, 527 (**2010**), 2265–2273, doi:10.1016/j.msea.2009.11.065

[12] X. Zhang, S. J. Lu, B. Zhang, X. B. Tian, Q. H Kan, G. Z. Kang, Dislocation–grain boundary interaction-based discrete dislocation dynamics modeling and its application to bicrystals with different misorientations, Acta Mater., 202 (**2021**), 88–98, doi:10.1016/j.actamat.2020.10.052

[13] A. Y. Zhang, R. Kang, L. Wu, H. C. Pan, H. B. Xie, Q. Y. Huang, Y. J. Liu, Z. R Ai, L. F. Ma, Y. P. Ren, G. W. Qin, A new rare-earth-free Mg-Sn-Ca-Mn wrought alloy with ultra-high strength and good ductility, Mater. Sci. Eng. A, 754 (**2019**), 269–274, doi:10.1016/j.msea.2019.03.095

[14] V. V. Karasiev, S. X. Hu, Unraveling the intrinsic atomic physics behind x-ray absorption line shifts in warm dense silicon plasmas, Phys. Rev. E, 103 (**2021**), 033202, doi:10.1103/PhysRevE.103.033202

[15] X. J. Zhang, F. Li, Y. Wang, C. Li, X. M. Xiao, Recrystallization behavior and texture evolution of magnesium alloy bending products under staggered extrusion, J. Mater. Eng. Perform., 30 (**2021**), 8108–8116, doi:10.1007/s11665-021-06056-w

[16] Q. Liu, L. M. Fang, Z. W. Xiong, J. Yang, Y. Tan, Y. Liu, Y. J. Zhang, Q. Tan, C. C. Hao, L. H. Cao, J. Li, Z. P. Gao, The response of dislocations, low angle grain boundaries and high angle grain boundaries at high strain rates, Mater. Sci. Eng. A, 822 (**2021**), 141704, doi:10.1016/j.msea.2021.141704

[17] Z. Y. Zhao, R. G. Guan, Y. F. Shen, P. K. Bai, Grain refinement mechanism of Mg-3Sn-1Mn-1La alloy during accumulative hot rolling, J. Mater. Sci. Technol., 91 (**2021**), 251–261, doi:10.1016/j.jmst.2021.02.052

[18] G. S. Zhang, Y. Z. Meng, F. F. Yan, Z. Gao, Z. M. Yan, Z. M. Zhang, Microstructure and texture evolution of Mg-RE-Zn alloy prepared by repetitive upsetting-extrusion under different decreasing temperature degrees, J. Alloys Compd., 815 (**2020**), 152452, doi:10.1016/j.jallcom.2019.152452

[19] Y. W. Gui, L. X. Ouyang, Y. J. Cui, H. K. Bian, Q. N. Li, A. Chiba, Grain refinement and weak-textured structures based on the dynamic recrystallization of Mg-9.80Gd-3.78Y-1.12Sm-0.48Zr alloy, J. Magnes. Alloy., 9 (**2021**), 456–466, doi:10.1016/j.jma.2020.06.001

[20] W. L. Xu, J. M. Yu, G. Q. Wu, L. C. Jia, Z. Gao, Z. Miao, Z. M. Zhang, Effect of decreasing temperature reciprocating upsetting-extrusion on microstructure and mechanical properties of Mg-Gd-Y-Zr alloy, Metals, 10 (**2020**), 1–11, doi:10.3390/met10070985

[21] X. X. Zhang, Y. Lv, T. Hashimoto, J. O. Nilsson, X. R. Zhou, Intergranular corrosion of AA6082 Al–Mg–Si alloy extrusion: The influence of trace Cu and grain boundary misorientation, J. Alloys Compd., 853 (**2021**), 157228, doi:10.1016/j.jallcom.2020.157228

[22] Y. D. Sun, W. Li, X. F. Shi, L. Tian, A uniformly fine-grained Mg-Y-Nd-Zr magnesium alloy with simultaneously optimized strength and ductility processed by forging and ECAP, Mater. Res. Express., 7 (**2020**), 116520, doi:10.1088/2053-1591/abc911